

See discussions, stats, and author profiles for this publication at: <https://www.researchgate.net/publication/231713583>

# Controllable Fabrication and Electrical Performance of Single Crystalline Cu<sub>2</sub>O Nanowires with High Aspect Ratios

ARTICLE *in* NANO LETTERS · NOVEMBER 2007

Impact Factor: 13.59 · DOI: 10.1021/nl0721259

CITATIONS

139

READS

71

6 AUTHORS, INCLUDING:



**Yiwei Tan**

Nanjing University of Technology

28 PUBLICATIONS 1,042 CITATIONS

SEE PROFILE



**Xinyu Xue**

Northeastern University (Shenyang, China)

82 PUBLICATIONS 2,304 CITATIONS

SEE PROFILE



**Taihong Wang**

Hunan University

279 PUBLICATIONS 12,260 CITATIONS

SEE PROFILE



**Yadong Li**

Tsinghua University

354 PUBLICATIONS 24,171 CITATIONS

SEE PROFILE

# Controllable Fabrication and Electrical Performance of Single Crystalline Cu<sub>2</sub>O Nanowires with High Aspect Ratios

Yiwei Tan,<sup>†</sup> Xinyu Xue,<sup>‡</sup> Qing Peng,<sup>†</sup> Heng Zhao,<sup>‡</sup> Taihong Wang,<sup>‡</sup> and Yadong Li<sup>\*,†</sup>

*Department of Chemistry, Tsinghua University, Beijing 100084, China, and Institute of Physics, Chinese Academy of Sciences, Beijing, 100080, China*

*Received August 23, 2007; Revised Manuscript Received October 31, 2007*

## ABSTRACT

We report a facile, solution-phase route to large-scale fabrication and characterization of single crystalline Cu<sub>2</sub>O nanowires with controllable diameter, different morphologies, and high aspect ratios. The synthesis of Cu<sub>2</sub>O nanowires is achieved by the reduction of cupric acetate with *o*-anisidine, pyrrole, or 2,5-dimethoxyaniline under hydrothermal conditions. The electrical properties of individual Cu<sub>2</sub>O nanowires have been examined by *I*–*V* characteristics. The output properties of Cu<sub>2</sub>O/poly(2,5-dimethoxyaniline) core/shell nanowires show n-type characteristics and improved conductivity, while those of Cu<sub>2</sub>O nanowires are linear. The results from this study provide a low-cost, naturally abundant nanostructured material for use in electronic devices.

Cuprous oxide (Cu<sub>2</sub>O) is a typical p-type direct band gap semiconductor with a band gap of 2.17 eV<sup>1</sup> and has potential applications in solar energy conversion,<sup>2</sup> electrode materials,<sup>3</sup> sensors,<sup>4</sup> and catalysis.<sup>5,6</sup> It has also been found that high-intensity photoexcitation can give rise to the coherent propagation of Cu<sub>2</sub>O excitons through Cu<sub>2</sub>O solid owing to the large exciton binding energy of 150 meV.<sup>7</sup> Single crystalline Cu<sub>2</sub>O with nanoscale dimensions could be anticipated to have spatially confined excitons and thereby increase their concentration. The large excitonic binding energy offers the possibilities to observe excitonic features in the absorption and luminescence spectrum.<sup>8,9</sup> Such unique electronic structures of Cu<sub>2</sub>O spur a growing amount of interest in its single crystalline nanostructures. Recently, different Cu<sub>2</sub>O nanostructures including nanospheres,<sup>9,10</sup> naocubes,<sup>11</sup> and nanowires,<sup>12,13</sup> have been synthesized with a variety of techniques.

One-dimensional (1D) nanomaterials such as nanowires,<sup>14</sup> nanotubes,<sup>15</sup> and nanobelts<sup>16</sup> are highly attractive building blocks for devices because of the inherent anisotropies and efficient transport of electrons and excitons within the smallest dimension. Although the electronic features of Cu<sub>2</sub>O determine that 1D Cu<sub>2</sub>O nanostructures are most promising for their use as components in nanoscale electronic devices, not until recently have limited techniques that allow one to prepare Cu<sub>2</sub>O nanowires been developed.<sup>12,13</sup> Cuprous oxide

is isotropic with a primitive cubic crystal structure. Thus, there are great challenges to achieve anisotropic growth of Cu<sub>2</sub>O molecules to form 1D single crystalline nanostructures in the absence of templates with 1D-confined structures. As a matter of fact, previous efforts on 1D Cu<sub>2</sub>O nanostructures yield polycrystalline, bent, entangled nanowires with low aspect ratios. Yet, the yields are not high.

Herein, we have developed novel solution-based syntheses of bulk quantities of single crystalline Cu<sub>2</sub>O nanowires with tunable diameter and morphology. We achieve uniform Cu<sub>2</sub>O nanowires in diameter through the reduction of cupric acetate (Cu(Ac)<sub>2</sub>) with *o*-anisidine, pyrrole, or 2,5-dimethoxyaniline as the reductant in dilute aqueous solutions under hydrothermal conditions. More importantly, the core/sheath structured Cu<sub>2</sub>O/poly(2,5-dimethoxyaniline) nanowires can be available in large quantities. The corresponding oxidative polymerizations of these monomers dictate the well-defined 1D growth of Cu<sub>2</sub>O single crystals. Consequently, no additional structure-directing reagents are required. In this work, we also demonstrate the electrical performances of individual Cu<sub>2</sub>O nanowire devices at different temperatures. The *I*–*V* characteristics of the Cu<sub>2</sub>O and Cu<sub>2</sub>O/poly(2,5-dimethoxyaniline) core/sheath nanowire devices were compared. Despite the ohmic behavior of Cu<sub>2</sub>O nanowires on gold contacts, the output properties of the single Cu<sub>2</sub>O/poly(2,5-dimethoxyaniline) nanowire devices exhibit n-type characteristics and enhanced conductivity.

**The Synthesis of Single Crystalline Cu<sub>2</sub>O Nanowires.** The redox reaction between Cu<sup>2+</sup> and the above-mentioned

\* To whom correspondence should be addressed.

<sup>†</sup> Department of Chemistry, Tsinghua University.

<sup>‡</sup> Institute of Physics, Chinese Academy of Sciences.

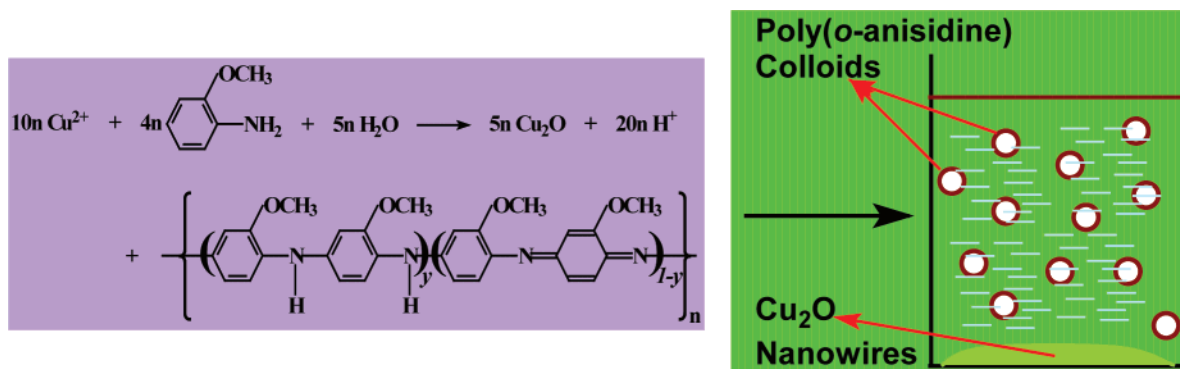


**Figure 1.** Schematic diagram depicting the formation process of Cu<sub>2</sub>O nanowires synthesized with *o*-anisidine as the reductant in autoclave.

monomers does not occur in dilute solutions of the starting reactants even at 120 °C and under normal atmospheric pressure because the oxidizing ability of the Cu<sup>2+</sup> ion is weak. To implement the redox reactions for the preparation of Cu<sub>2</sub>O nanowires, the experiments should be carried out at temperatures above 110 °C under hydrothermal conditions. Typically, 0.10–0.30 g of Cu(Ac)<sub>2</sub> was dissolved in 40 mL of deionized water. Afterward, to this solution was added 10 mL of an aqueous solution of *o*-anisidine or pyrrole (0.10 M), which invokes the reaction mixture to become dark green or olive green owing to the coordination of Cu<sup>2+</sup> and *o*-anisidine or pyrrole. The reaction mixture was transferred to a 50 mL autoclave. The autoclave was sealed and maintained at 140–180 °C for 10 h or at 250 °C for 5 h and subsequently cooled to ambient temperature naturally. In the case of the reductant 2,5-dimethoxyaniline, the synthetic procedure is similar to that described above. However, taking the low solubility of 2,5-dimethoxyaniline in water at ambient temperature into account, 2 mmol of 2,5-dimethoxyaniline was dissolved in 40 mL of heat-deionized water (60 °C), and then 10 mL of 0.05 M Cu(Ac)<sub>2</sub> was added. This reaction mixture was loaded in an autoclave and maintained at 180 °C for 10 h.

Interestingly, the oxidative polymerization initiated by Cu<sup>2+</sup> results in poly(*o*-anisidine), poly(pyrrole), or poly(2,5-dimethoxyaniline) forming stable colloidal solution. The as-prepared Cu<sub>2</sub>O nanowires are in the form of yellow green or brown (using *o*-anisidine (250 °C) or 2,5-dimethoxyaniline as the reductant) sediments at the bottom of autoclave. Particularly, when *o*-anisidine is used as the reductant, voided or solid spherical poly(*o*-anisidine) colloids are yielded.<sup>17</sup> Figure 1 depicts the chemical reaction equation and the distribution of the products in the reaction vessel. The sediments (Cu<sub>2</sub>O nanowires) could be readily isolated by pouring off the supernatant colloidal polymer solution. The isolated sediments were washed with ethanol for many times and dried.

Figure 2 shows the powder X-ray diffraction (XRD) pattern of the sediments obtained with *o*-anisidine as the reductant, in which a set of Bragg peaks can be perfectly indexed as the pure cubic cuprite structure (*Pn* $\bar{3}$ *m*, JCPDF no. 78–2076) with lattice constant *a* = 4.267 Å. Scanning electron microscopy (SEM) overviews reveal that the Cu<sub>2</sub>O sediments are long, straight nanowires (Figure 3a). The length

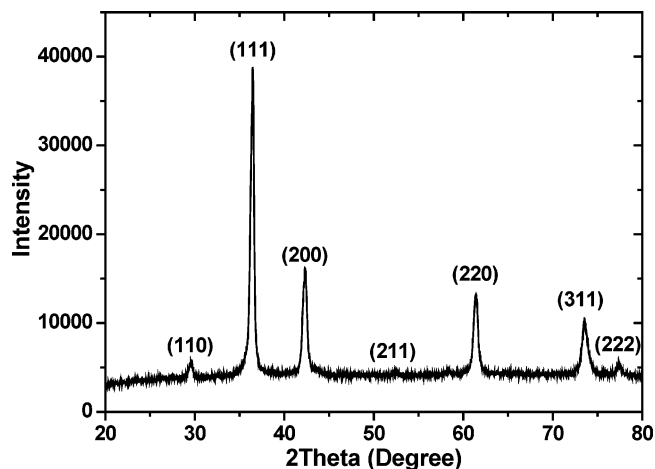


**Figure 2.** Powder X-ray diffraction pattern of the as-prepared Cu<sub>2</sub>O nanowires.

of the Cu<sub>2</sub>O nanowires ranges from tens of micrometers to more than a hundred micrometer. The corresponding transmission electron microscopy (TEM) image in Figure 3c displays that the diameters of the Cu<sub>2</sub>O nanowires are typically 40–70 nm and uniform along their length. In addition, small burrs grow on the surfaces of Cu<sub>2</sub>O nanowires. Such branched nanowires are highly desirable for the improvement of the performance of nanowire-based sensors<sup>18</sup> and photovoltaic devices<sup>19</sup> owing to an increase in the wire surface area. The nanowires' length and diameter are independent of hydrothermal reaction time and temperature. The yield of the reaction at 140–180 °C is ca. 85% based on the weight of the isolated nanowires, and the reaction can be easily scaled up to gram scale as 1.0 g of nanowires can be obtained from a 500 mL synthesis by the reduction of 0.038 M Cu(Ac)<sub>2</sub> with 0.02 M *o*-anisidine. Surveys of numerous samples synthesized at different temperatures using selected area electron diffraction (SAED) and high-resolution TEM (HRTEM) indicate that the Cu<sub>2</sub>O nanowires are consistently single crystal. HRTEM images reveal most nanowires with well-resolved (111) and (110) lattice planes (Figure 3d,e). The insets in Figure 3d,e illustrate the corresponding SAED patterns. HRTEM and the assignments of SAED consistently indicate that the preferential growth direction for Cu<sub>2</sub>O nanowires is [110].

In contrast, the morphology of Cu<sub>2</sub>O nanowires changes as increasing the reaction temperature to 250 °C, while the



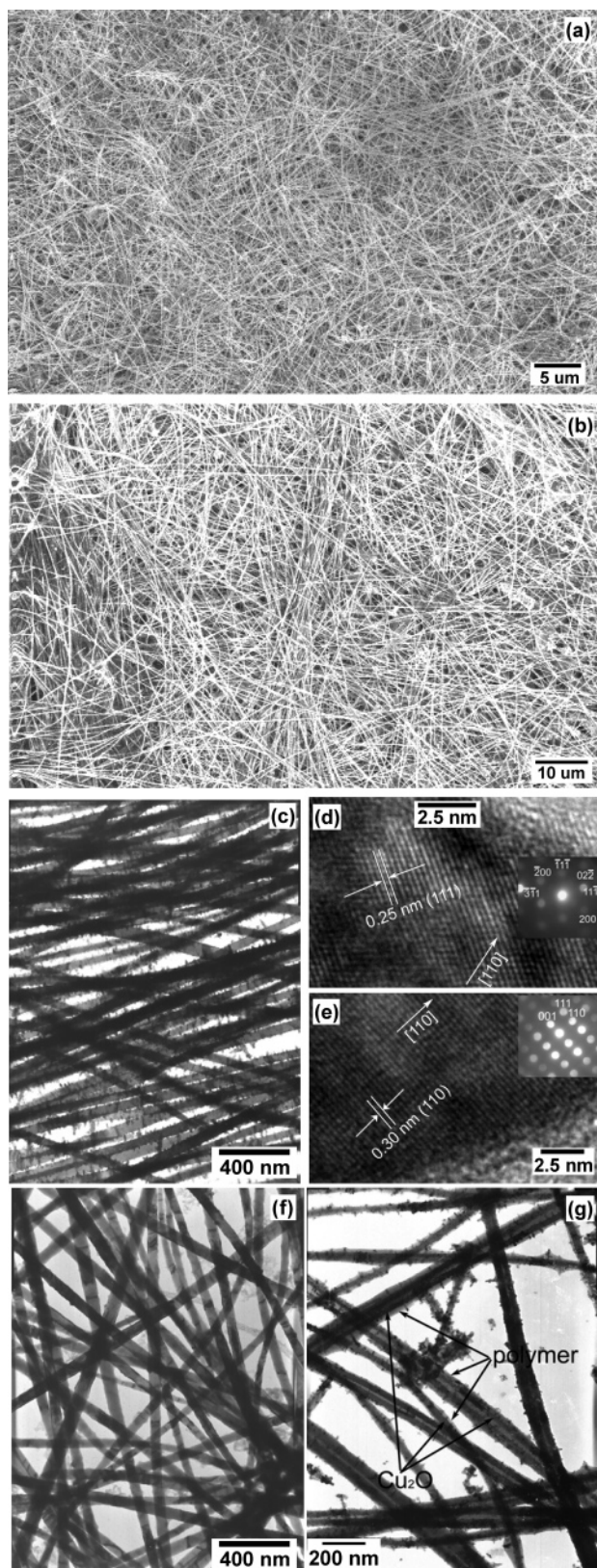


**Figure 3.** SEM images of  $\text{Cu}_2\text{O}$  nanowires synthesized at 180 °C with (a) *o*-anisidine and (b) pyrrole as the reductant. (c) TEM and (d,e) HRTEM images of the  $\text{Cu}_2\text{O}$  nanowires from the sample in panel a. The insets show the corresponding SAED patterns. (f) TEM image of  $\text{Cu}_2\text{O}$  nanowires synthesized at 250 °C with *o*-anisidine as the reductant. (g) TEM image of  $\text{Cu}_2\text{O}$ /poly(2,5-dimethoxyaniline) core/sheath nanowires synthesized at 180 °C with 2,5-dimethoxyaniline as the reductant.

length and diameter of the nanowires remain unchanged. The surface of the  $\text{Cu}_2\text{O}$  nanowires becomes smooth because no burrs grow on the nanowires (Figure 3f). The goal of this synthesis is that straight nanowires with minimal surface roughness may be useful as high-performance FETs for the high carrier mobilities.<sup>20</sup> Likewise, XRD measurements, TEM observations, and ED patterns confirm that single crystalline  $\text{Cu}_2\text{O}$  nanowires are also available in bulk quantities with pyrrole or 2,5-dimethoxyaniline as the reducing reagent. If pyrrole is utilized as the reductant, the diameter of the  $\text{Cu}_2\text{O}$  nanowires increases to 130–170 nm (Figure 3b). It can also be seen that the length of most  $\text{Cu}_2\text{O}$  nanowires exceeds one hundred micrometers. In particular, use of the reductant 2,5-dimethoxyaniline allows us to synthesize  $\text{Cu}_2\text{O}$ /poly(2,5-dimethoxyaniline) core/sheath nanowires (Figure 3g). The core/sheath nanowires are tens of micrometers in length with a 20–50 nm diameter core of  $\text{Cu}_2\text{O}$  and a 2–25 nm thick outer sheath of polymer. The  $\text{Cu}_2\text{O}$  core can be etched out with 1.0 M hydrochloric acid over 9 h, leading to yielding poly(2,5-dimethoxyaniline) nanotubes in the form of precipitates. The TEM image in Figure 4a clearly demonstrates the tubular morphology of poly(2,5-dimethoxyaniline). The outer diameter and wall thickness are 30–70 and 5–15 nm, respectively, in good agreement with the corresponding values obtained from Figure 3g. The Fourier transform infrared (FT-IR) spectrum confirms that this tubular polymer is in the form of emeraldine base, as shown in Figure 4b.<sup>21</sup>

Concerning the anisotropic growth mechanism for the formation of single crystalline  $\text{Cu}_2\text{O}$  nanowires, we suggest that the polymers formed in situ selectively adsorb onto the crystallographic planes of  $\text{Cu}_2\text{O}$ . We speculate that the adsorption of the polymers on  $\text{Cu}_2\text{O}$  crystallites is based on the chemical interaction between the given  $\text{Cu}_2\text{O}$  facets and the ligand amine group ( $-\text{NH}-$ ). However, our studies reveal that not all derivatives of *o*-anisidine are effective in producing  $\text{Cu}_2\text{O}$  nanowires. Instead, when aniline, 2-methylaniline, or 2,6-dimethylaniline is used as the reductant under otherwise conditions identical with those for synthesizing  $\text{Cu}_2\text{O}$  nanowires, spherical  $\text{Cu}_2\text{O}$  nanoparticles with diameters of 3–20 nm are obtained. Therefore, the key to controlling 1D growth of the  $\text{Cu}_2\text{O}$  nanocrystals is the type/site of ortho-group in the reductants. The size and/or position of ortho-group related to the ligand amine group can determine the selectivity of the polymer adsorption due to the steric effects. Note that the diameter of the  $\text{Cu}_2\text{O}$  nanowires decreases with the increase of the number of methoxy group in the reductant molecules (i.e., the  $-\text{OCH}_3$  number ratio of pyrrole/*o*-anisidine/2,5-dimethoxyaniline is 0:1:2). This result indicates that increasing the number of methoxy group makes the steric effects more intensive, being responsible for the higher adsorption selectivity. Accordingly, the growth of the given  $\text{Cu}_2\text{O}$  facets is effectively suppressed. On the other hand, this means the stronger chemical adsorption of the amine group on the  $\text{Cu}_2\text{O}$  facets due to the donating electron effect of the methoxy group thus further suppressing the transverse growth of the  $\text{Cu}_2\text{O}$  nanowires. It is the reason why the  $\text{Cu}_2\text{O}$ /poly(2,5-dimethoxyaniline)

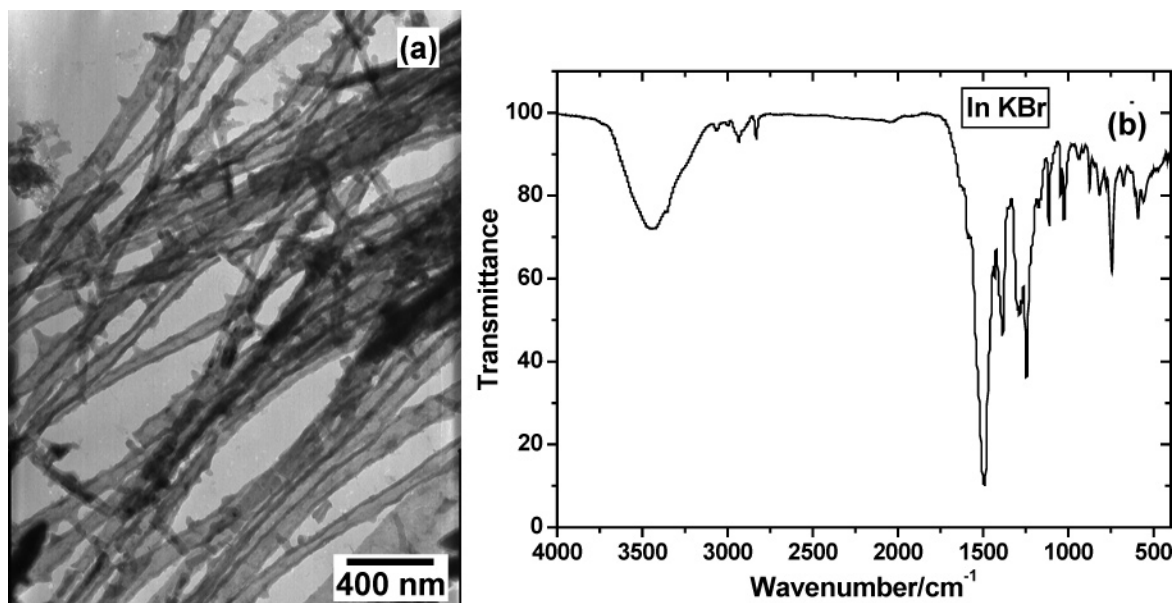


**Figure 4.** (a) TEM image of poly(2,5-dimethoxyaniline) nanotubes obtained after etching out the  $\text{Cu}_2\text{O}$  nanowire cores. (b) FT-IR spectrum of poly(2,5-dimethoxyaniline) nanotubes.

core/sheath nanowires are formed after 2,5-dimethoxyaniline is polymerized to give two *ortho*-methoxy groups on each segment of a pair of amine-linked benzene rings.

**The Electrical Transport Properties.** Typically, the electrical transport properties of the single crystalline  $\text{Cu}_2\text{O}$  nanowires prepared with *o*-anisidine as the reductant at 180 °C were studied on devices consisting of individual nanowires. A standard electron-beam lithography technique was used to design pairs of metal electrodes on a silicon substrate capped with a 50 nm silicon dioxide layer (the  $\text{SiO}_2/\text{Si}$  substrate), followed by metal deposition of Ti/Au (10 nm/100 nm) by electron beam evaporation to complete the device structure. The  $\text{Cu}_2\text{O}$  nanowires were transferred onto the prefabricated electrodes by touching the nanowire sample with the electrodes, by which only a single  $\text{Cu}_2\text{O}$  nanowire lying across two electrodes can be easily made. The electrical properties of individual nanowires in more than 20 devices were investigated in vacuum ( $1.0 \times 10^{-3}$  Pa) at room temperature and high temperatures. A linear current ( $I_{\text{ds}}$ ) versus voltage ( $V_{\text{ds}}$ ) curve was observed in all devices measured, indicating the ohmic nature of the contact with Au electrode. For a p-type  $\text{Cu}_2\text{O}$  semiconductor, the ohmic contact is due to the work function of the contact metal (Au), which is larger than that of  $\text{Cu}_2\text{O}$ .<sup>22</sup> Figure 5a illustrates the  $I_{\text{ds}}-V_{\text{ds}}$  curves from a randomly selected sample at different temperatures. The inset of Figure 5a shows a SEM image of a bottom-contact  $\text{Cu}_2\text{O}$  nanowire device in which a  $\text{Cu}_2\text{O}$  nanowire spans the source-drain gold electrodes. By means of the measured resistance value of the device, the cross-section size (73 nm), and the length (1.3  $\mu\text{m}$ ) of the  $\text{Cu}_2\text{O}$  nanowire (measured by SEM imaging), we can calculate the resistivity to be  $4.7 \times 10^4$ ,  $1.8 \times 10^4$ , and  $0.8 \times 10^4 \Omega\cdot\text{cm}$  at 298, 373, and 450 K, respectively. It can be seen that the resistivity of  $\text{Cu}_2\text{O}$  nanowires decreases with increasing temperature. This variance trend of resistivity with temperature is observed in all  $\text{Cu}_2\text{O}$  nanowire devices. This behavior

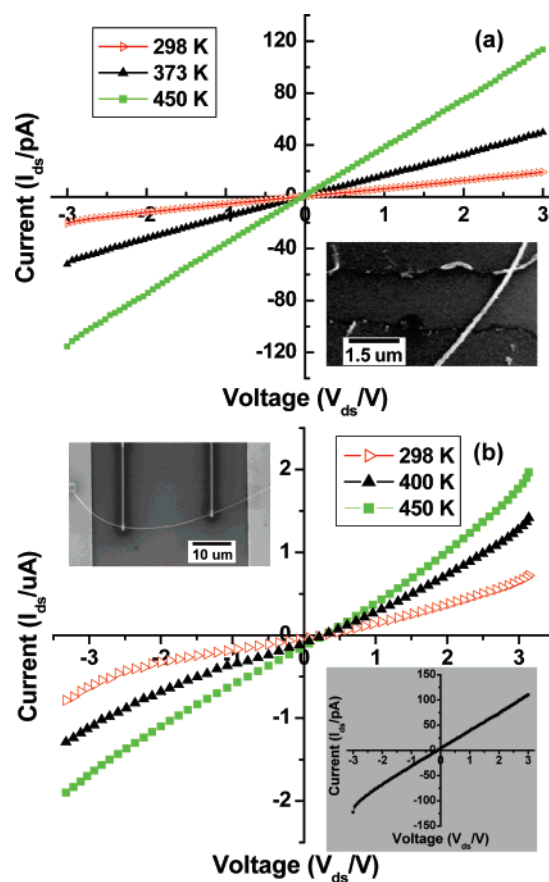


**Figure 5.**  $I_{\text{ds}}-V_{\text{ds}}$  characteristics of (a) an individual single crystalline  $\text{Cu}_2\text{O}$  nanowire and (b) an individual  $\text{Cu}_2\text{O}$ /poly(2,5-dimethoxyaniline) core/sheath nanowire device measured at different temperatures. Insets in panels a and b are the SEM images of a  $\text{Cu}_2\text{O}$  nanowire and a  $\text{Cu}_2\text{O}$ /poly(2,5-dimethoxyaniline) core/sheath nanowire device and the room-temperature  $I_{\text{ds}}-V_{\text{ds}}$  curve of poly(2,5-dimethoxyaniline) nanotubes, respectively.

is consistent with the expected resistivity–temperature relationship for semiconductors.



When the same bias was applied to a Cu<sub>2</sub>O/poly(2,5-dimethoxyaniline) core/sheath nanowire device at different temperatures, nonlinear n-type  $I_{ds}$ – $V_{ds}$  characteristics and increased electric conductivity were observed, as shown in Figure 5b.<sup>23</sup> To reduce the contact resistance, individual Cu<sub>2</sub>O/poly(2,5-dimethoxyaniline) nanowires were contacted with four platinum pad electrodes (0.8  $\mu$ m thick) that were fabricated on a SiO<sub>2</sub> (500 nm)/Si substrate by using focused ion-beam-induced platinum deposition (Figure 5b, upper left inset). The observed conductivity of the Cu<sub>2</sub>O/poly(2,5-dimethoxyaniline) nanowire increases with temperature and is several orders higher than that of the Cu<sub>2</sub>O nanowires. Compared to the single Cu<sub>2</sub>O nanowire device, these changes were detected in 80% of over 20 measured Cu<sub>2</sub>O/poly(2,5-dimethoxyaniline) nanowire devices. To understand the changes, we also examine the  $I_{ds}$ – $V_{ds}$  characteristics of the poly(2,5-dimethoxyaniline) nanotubes prepared by etching out Cu<sub>2</sub>O nanowires. The curve illustrates that the electrical behavior of the poly(2,5-dimethoxyaniline) nanotubes treated by HCl is similar to that of single crystalline Cu<sub>2</sub>O nanowires (Figure 5b, lower right inset). Therefore, the enhanced conductivity and the change of output properties of the Cu<sub>2</sub>O/poly(2,5-dimethoxyaniline) nanowires compared to pure Cu<sub>2</sub>O nanowires may not result from the poly(2,5-dimethoxyaniline) shell itself.

The improved electrical properties of the Cu<sub>2</sub>O/poly(2,5-dimethoxyaniline) nanowires may be attributed to the covalent bonding between the active amine group of poly(2,5-dimethoxyaniline) and Cu<sub>2</sub>O as well as the conjugated segments comprised of continuous overlapping orbits (N=Q=N, Q = quinoid ring) in the polymer backbone, which act as the electron donors. As a result, poly(2,5-dimethoxyaniline) can provide electrons to the inner Cu<sub>2</sub>O nanowires to produce an abundance of mobile or “carrier” electrons in the material. At this point, electrons are the majority carriers. Consequently, the Cu<sub>2</sub>O/poly(2,5-dimethoxyaniline) nanowires exhibit the electrical properties of an n-type semiconductor. Actually, the increased conductivity may be also associated with the coating of the polymer. In a recent report by Wong and Wang et al.,<sup>24</sup> the increased conductivity of the organic molecules modified ZnO nanobelts was demonstrated. They proposed that the enhancement in conductivity of the ZnO nanobelts treated with small organic molecules is due to the decreases of both Schottky barrier height and the contact resistance on the basis of the formation of dipole. In our experiments, a dipole may likewise form at the interface of Cu<sub>2</sub>O/polymer as a consequence of the covalent bonding between them.<sup>25</sup> Such a dipole layer can reduce Schottky barrier height and mediate the transport of electrons from the metal contact to semiconductor, leading to a remarkable decrease in the contact resistance. On the other hand, the presence of electron donors, that is, amine groups and the extended delocalized bonds in poly(2,5-dimethoxyaniline) chains, increases the carrier density, thereby inducing a further increase in conductance.

In conclusion, we have described solution-phase syntheses of single crystalline Cu<sub>2</sub>O nanowires under hydrothermal conditions, which have the merits of low-cost, large-scale

production, and facile manipulation. The diameter and morphology of Cu<sub>2</sub>O nanowires can be easily tuned by the choice of reductant type and synthetic temperature. Moreover, the unique Cu<sub>2</sub>O/poly(2,5-dimethoxyaniline) core/sheath nanowires are fabricated. The electrical transport properties of the as-synthesized single crystalline Cu<sub>2</sub>O and Cu<sub>2</sub>O/poly(2,5-dimethoxyaniline) core/sheath nanowires present ohmic and n-type characteristics, respectively. The conductivity of the Cu<sub>2</sub>O/poly(2,5-dimethoxyaniline) nanowires is dramatically enhanced in comparison to that of single crystalline Cu<sub>2</sub>O nanowires. The coating of poly(2,5-dimethoxyaniline) sheath plays an important role in varying electrical output properties of the Cu<sub>2</sub>O nanowires. Such single crystalline Cu<sub>2</sub>O nanowires are very desirable in field-effect transistor applications.

**Acknowledgment.** We thank Dr. Zhimin Liao and Professor Dapeng Yu of Peking University for the assistance with fabrication and measurements of four-probe devices. We gratefully acknowledge the financial support of NSFC (90606006), the State Key Project of Fundamental Research (2006CB932300), and the Key Grant Project of Chinese Ministry of Education (No. 306020)

## References

- (1) Agekyan, V. T. *Phys. Status Solidi A* **1977**, *43*, 11.
- (2) Musa, A. O.; Akomolafe, T.; Carter, M. J. *Sol. Energy Mater. Sol. Cells* **1998**, *51*, 305.
- (3) Poizot, P.; Laruelle, S.; Grugeon, S.; Dupont, L.; Taramon, J. M. *Nature (London)* **2000**, *407*, 496.
- (4) Zhang, J.; Liu, J.; Peng, Q.; Wang, X.; Li, Y. *Chem. Mater.* **2006**, *18*, 867.
- (5) de Jongh, P. E.; Vanmaelkelbergh, D.; Kelly, J. J. *Chem. Commun.* **1999**, 1069.
- (6) White, B.; Yin, M.; Hall, A.; Le, D.; Stolbov, S.; Rahman, T.; Turro, N.; O'Brien, S. *Nano Lett.* **2006**, *6*, 2095.
- (7) Snoke, D. *Science* **1996**, *273*, 1351.
- (8) Caswell, N.; Yu, P. Y. *Phys. Rev. B* **1982**, *25*, 5519.
- (9) Deki, S.; Akamatsu, K.; Yano, T.; Mizuhata, M.; Kajinami, A. *J. Mater. Chem.* **1998**, *8*, 1865.
- (10) (a) Rockenberger, J.; Scher, E. C.; Alivisatos, A. P. *J. Am. Chem. Soc.* **1999**, *121*, 11595. (b) Borgohain, K.; Murase, N.; Mahamuni, S. *J. Appl. Phys.* **2002**, *92*, 1292. (c) Yin, M.; Wu, C.-K.; Lou, Y.; Burda, C.; Koberstein, J. T.; Zhu, Y.; O'Brien, S. J. *Am. Chem. Soc.* **2005**, *127*, 9506.
- (11) Gou, L.; Murphy, C. J. *J. Mater. Chem.* **2004**, *14*, 735.
- (12) Wang, W.; Wang, G.; Wang, X.; Zhan, Y.; Liu, Y.; Zheng, C. *Adv. Mater.* **2002**, *14*, 67.
- (13) Singh, D. P.; Neti, N. R.; Sinha, A. S. K.; Srivastava, O. N. *J. Phys. Chem. C* **2007**, *111*, 1638.
- (14) (a) Duan, X.; Huang, Y.; Cui, Y.; Lieber, C. M. *Molecular Nanoelectronics*; Reed, M. A., Lee, T., Eds.; American Scientific Publishers: Stevenson Ranch, CA, 2003. (b) Lieber, C. M. *Solid State Commun.* **1998**, *107*, 607. (c) Zhong, Z.; Fang, Y.; Lu, W.; Lieber, C. M. *Nano Lett.* **2005**, *5*, 1143.
- (15) (a) Tans, S. J.; Verschueren, A. R. M.; Dekker, C. *Nature (London)* **1998**, *393*, 49. (b) Hu, C.-C.; Chang, K.-H.; Lin, M.-C.; Wu, Y.-T. *Nano Lett.* **2006**, *6*, 2690.
- (16) Arnold, M. S.; Avouris, P.; Pan, Z. W.; Wang, Z. L. *J. Phys. Chem. B* **2003**, *107*, 659.
- (17) Tan, Y.; Bai, F.; Wang, D.; Peng, Q.; Wang, X.; Li, Y. *Chem. Mater.* **2007**, *19*, 5773.
- (18) Patolsky, F.; Zhang, G.; Hayden, O.; Lakadamyali, M.; Zhuang, X.; Lieber, C. M. *Proc. Natl. Acad. Sci. U.S.A.* **2004**, *101*, 14017.
- (19) Huynh, W. U.; Dittmer, J. J.; Alivisatos, A. P. *Science* **2002**, *295*, 2425.
- (20) Cui, Y.; Zhong, Z.; Wang, D.; Wang, W. U.; Lieber, C. M. *Nano Lett.* **2003**, *3*, 149.

- (21) The N–H stretching peaks are observed at 3300–3500  $\text{cm}^{-1}$ . The absorption bands related to the quinoid ring and stretching of benzenoid ring appear at 1580 and 1490  $\text{cm}^{-1}$ , respectively. The bands at 1286 and 1245  $\text{cm}^{-1}$  originate from C–N and C–O stretching absorptions, respectively. The bands at 1386, 2832, and 2935  $\text{cm}^{-1}$  are due to the  $-\text{CH}_3$  substituted group, while the bands at 3000 and 3065  $\text{cm}^{-1}$  can be assigned to the C–H stretch of benzenoid ring. In addition, the bands at 1000–400  $\text{cm}^{-1}$  are associated with the 2,5-substituted aromatic rings.
- (22) Wang, D.; Lu, J. G.; Otten, C. J.; Buhro, W. E. *Appl. Phys. Lett.* **2003**, 83, 5280.
- (23) When the work function of the contact metal is larger than that of the semiconductor, an n-type semiconductor exhibits a Schottky barrier while a p-type semiconductor exhibits ohmic contact. The work function (WF) of poly(2,5-dimethoxyaniline) is not larger than that of polyaniline (4.5–4.7 eV) due to the donating electron effect of methoxy group. Thus, Schottky barriers existing between the  $\text{Cu}_2\text{O}$ /poly(2,5-dimethoxyaniline) nanowires and the Pt (WF, 5.7 eV) contacts implies that the  $\text{Cu}_2\text{O}$ /poly(2,5-dimethoxyaniline) core/sheath nanowires are an n-type semiconductor. Also see: (a) Posdorfer, J. R.; Werner, B.; Wessling, B.; Heun, S.; Becker, H. *Proc. SPIE-Int. Soc. Opt. Eng.* **2004**, 5214, 188. (b) Huang, Y.; Yue, S.; Wang, Z.; Wang, Q.; Shi, C.; Xu, Z.; Bai, X. D.; Tang, C.; Gu, C. *J. Phys. Chem. B* **2006**, 110, 796.
- (24) Lao, C.; Li, Y.; Wong, C. P.; Wang, Z. L. *Nano Lett.* **2007**, 7, 1323.
- (25) de Boer, B.; Hadipour, A.; Mandoc, M. M.; van Woudenberg, T.; Blom, P. W. M. *Adv. Mater.* **2005**, 17, 621.

NL0721259